# Evaluation of E-field distributions in parallel transmit systems by time-domain optical electric-field sensors

**F. Seifert**[1]**, T. D. Lindel**[1]**, and P. Ullmann**[2]
[1]Physikalisch-Technische Bundesanstalt (PTB), Abbestr. 2-12, D-10587 Berlin, Germany, [2]Bruker BioSpin MRI GmbH, Ettlingen, Germany

## Introduction and Motivation

Ensuring RF safety is crucial for parallel transmission in MRI. In general, during parallel transmission the E-field distributions inside and outside the body exhibit a complex time evolution which cannot be covered by calorimetric SAR measurements. Furthermore, the knowledge of E-field evolution at selected positions would afford a better understanding of the complicated interaction of transmitting coil elements. To this end, we propose to utilize a time domain sensor to record the time evolution of the complex-valued E-field vector during multi-dimensional RF pulses. We applied a customized all optical E-field sensor which features full compatibility to the MR system. In first experiments a 4-channel transmit system at 3T was used to generate various well defined $B_1^{(+)}$ and SAR distributions in a phantom designed to accommodate the sensor head.

## Materials and Methods

The optical electric field sensor (OEFS) system (Seikoh Giken OEFS-S1B) consists of a 12 mm diameter sensor head and a controller unit (Fig.1). The sensor head comprises 3 Mach-Zehnder-type electro-optic E-field sensor chips which are coupled to the controller by optical fibers with a length of 10 m. The long axis of the head is aligned with the space diagonal of the sensor's coordinate system which has to be taken into account when transforming the data into the laboratory frame. The signal from each sensor chip is optically switched to the photo detector. The amplified RF signal (bandwidth 3 GHz) from the controller is recorded by a 2 channel digital radio PCI card (Echotek ECDR-GC314-PCI) operating at the MR-scanner's (Bruker MedSpec 30/100) frequency of 125.3 MHz. This data acquisition card is synchronized by an 80 MHz clock signal from the scanner and triggered by a TTL-signal generated by the MR sequence. One channel is used for recording the OEFS signal, the other one records the transmitted RF pulse signal delivered by a directional coupler. In this way a stable phase reference can be established. The cylindrical phantom (d = l = 20 cm) was filled with water which was doped with 0.66 g/l $CuSO_4$ and 1.33 g/l NaCl (Fig.2). The phantom has 4 through-going tubes to accommodate the sensor head mount. This mount allows for adjusting the z-position and the angle within the transversal plane. By rotating the whole phantom circular plots of the E-field distribution can be measured, in this study only the most outward sensor channel was used. The 4-channel transmit/receive coil array based on current sheet antennae (CSA) is described in [1]. Since for this geometry the E-field vector has no transversal components in the central axial plane, no permittivity correction of the E-field data has to be considered. $B_1^{(+)}$-maps were acquired by a saturation pulse sequence as described in [1]. $\vec{E}\cdot\vec{E}^*$ as SAR-analogon was calculated from the average of 100 individual RF pulses acquired during the first part of a gradient echo sequence with 256 phase encoding steps.

## Results

For our setup we used a special phase setting which was known to produce a single hot-spot SAR-distribution [1]. We applied the following phases to the 4 transmit elements: 0°(anterior)-135°(right)-0°(posterior)-270°(left), the applied transmit amplitudes were the same for all elements. In Fig.3 the results of the $B_1^{(+)}$- and E-field measurements as well as FDTD simulations from [1] are shown. The measured $B_1^{(+)}$-maps coincide well with the simulated distributions (note the signal voids at the location of the sensor channels and one spot of very low transmit field amplitude). The same holds for the measured $\vec{E}\cdot\vec{E}^*$ circular plot and the simulated SAR distribution as expected from electrodynamics. Since the OEFS was not calibrated, we present relative data only. However, after calibration the method is fully quantitative.

Fig.1: customized 3-axis OEFS-System

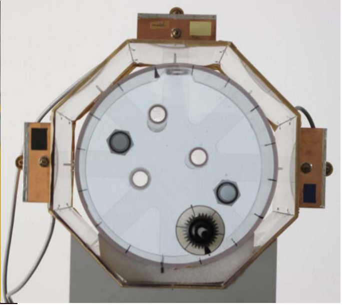

Fig.2: 4-channell CSA-array and phantom with 4 tubes for OEFS

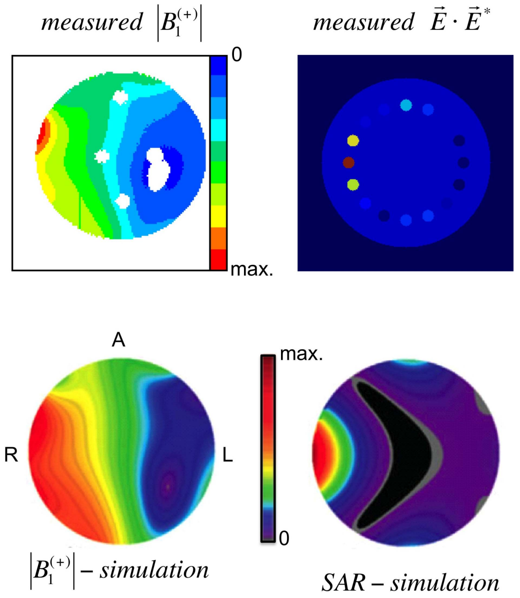

Fig.3: 4-channel static phase transmission: Comparison of measured transmit fields and OEFS-measurements with corresponding FDTD simulations (note different types of color scales).

## Conclusions

We introduced an optical electric field sensor to map non-stationary E-field distributions in real time during parallel transmit MRI. Within a feasibility study we tested the experimental setup for a 4-channel transmit array and a certain static phase setting. Our measurements confirmed a pathologic single hot-spot SAR-distribution as expected from FDTD simulations. In conclusion, the featured OEFS, in conjunction with FDTD-simulations, $B_1$-measurements and calorimetric SAR measurements, can be an appropriate tool to identify, in particular, possible safety issues of parallel transmit technologies.

This work is a part of the INUMAC project supported by the German Federal Ministry of Education and Research, grant #13N9207.

## References

[1] F. Seifert, G. Wuebbeler, S. Junge, B. Ittermann, and H. Rinneberg, JMRI 26 (2007) 1315-1321